

Fluctuations at the Base Pair Level Effecting Charge Transfer in DNA[†]Sairam S. Mallajosyula,[‡] Ashutosh Gupta,[§] and Swapan K. Pati^{*,‡}*Theoretical Sciences Unit and DST Unit on Nanoscience, Jawaharlal Nehru Center for Advanced Scientific Research, Jakkur Campus, Bangalore 560 064, India, and Department of Chemistry, Udai Pratap Autonomous College, Varanasi, Uttar Pradesh 221002, India*

Received: November 20, 2008; Revised Manuscript Received: December 23, 2008

We investigate the energetics of the basepair degrees of freedom and their effects on the overall charge transfer processes in DNA. We find that the rotational and translational basepair degrees of freedom can be broadly classified into soft and hard vibrational modes, with the stiffness of the modes depending on the nature of the basepair. We also find that the intrabasepair charge transfer, in the A:T and G:C basepairs, is strongly influenced by open (σ) and stretch (S_y) vibrational modes. Our calculations for the AT–GC and GC–AT dinucleotide steps suggest that the fluctuations in the G:C basepair strongly influence the site energies when compared to fluctuations in the A:T basepair. However, for both the dinucleotide steps, we find that the charge transfer integrals are strongly influenced by the fluctuations at the basepair level. Overall, our studies suggest that for a better understanding of the overall charge transfer processes, it is important to account for the basepair fluctuations.

1. Introduction

Nucleic acids undergo a wide variety of thermally induced fluctuations that occur on time scales ranging from picoseconds to milliseconds and with spatial extents ranging from fractions of an angstrom to tens of angstroms.^{1,2} These fluctuations have been found to play an important role in the biological functioning of the nucleic acids. In particular, it has been found that fluctuations in local helical conformation, which occur on the picosecond to nanosecond time scale, play a significant role in specific protein–DNA binding by enabling proteins to indirectly probe the base sequence via local changes in mechanical and dynamic behavior.^{3–5} It has also been found that base pair disruption is a necessary step in making reactive sites on the bases accessible for chemical attack. Specifically, it has been found that base opening, i.e., the movement of at least one base out of helical stack via the destruction of Watson–Crick hydrogen bonding within a base pair, is an intrinsic part of enzyme-catalyzed DNA modifications, such as selective methylation.⁶ In recent years, both experimental and computational studies have also revealed the importance of conformational dynamics of the DNA basepairs effecting the rates of hole transfer in DNA.^{7–11} It has been shown that the hole-transfer dynamics exhibit a strong dependence on the twist angle (defined as the relative twist between consecutive basepair steps) and the rise (defined as the relative distance between consecutive basepair steps) for a particular DNA sequence.^{7,9}

It is to be noted that these fluctuations occur in DNA at two distinct levels, the basestep level and the basepair level. The energetics of the two classes of fluctuations differ due to the different forces that are involved in stabilizing them. While the basestep is stabilized by the interbase π – π interactions, the basepair is stabilized through interbase hydrogen bonding (H-bond). These fluctuations are classified by six degrees of freedom in both the cases (Figure 1). At the basestep level, the

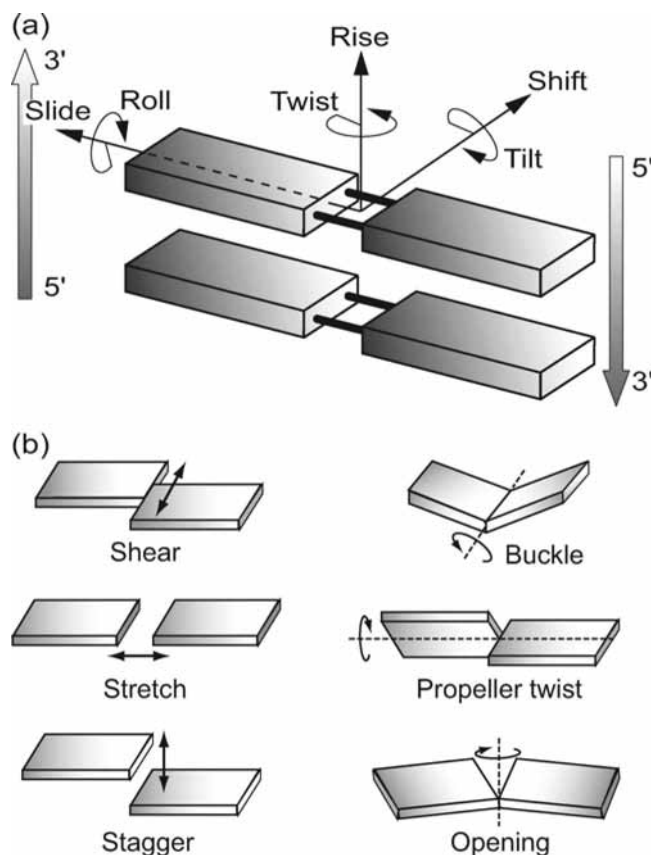


Figure 1. Translational and rotational degrees of freedom at the (a) basestep level and (b) basepair level.

conformational space is described by three translational [shift (D_x), slide (D_y), and rise (D_z)] and three rotational [tilt (τ), roll (ρ), and twist (Ω)] degrees of freedom, while at the basepair level, the conformational space is described by the translational [stagger (S_z), stretch (S_y), and shear (S_x)] and rotational [propeller twist (ω), buckle (κ), and open (σ)] degrees of freedom.¹²

[†] Part of the George C. Schatz Festschrift.

* Corresponding author. E-mail: pati@jncasr.ac.in.

[‡] Jawaharlal Nehru Center for Advanced Scientific Research.

[§] Udai Pratap Autonomous College.

While a large number of computational studies have been devoted to study DNA deformity at the dinucleotide level (basestep level),^{9,11,13} there have not been many studies on analyzing the deformity at the basepair level. In fact, the majority of theoretical studies discussing the energetics of the H-bonds in DNA basepairs treat the basepair as a rigid planar unit.^{14,15} While, an analysis of the crystallographic data for DNA oligomers demonstrates that the DNA basepairs are often not planar but distorted.¹⁶ From crystal database analysis and molecular dynamics simulations, it has also been shown that the magnitude of the intrabasepair distortions are quite comparable to the interbasepair fluctuations.^{17–19} In a recent theoretical report, it has been shown that individual nucleobase motions also effect the hole transfer rates.²⁰ To the best of our knowledge, there have been only a very few investigations into the energetics of the basepair deformations and in turn their effects on structural stability and charge transfer. In fact, recent calculations using QM/MD (quantum mechanics/molecular dynamics) simulations on the DNA hairpin and PNA (peptide nucleic acid) structures have highlighted the role of structural fluctuations affecting the hole transport in these structures.^{21–23} In these studies, the authors used molecular dynamics trajectories for the QM studies, thus sampling the thermal fluctuations in the DNA structures. It was found that these thermal fluctuations strongly affect hole-transfer processes. However, in all of these studies the results suggested no direct correspondence with the DNA basepair/basestep degrees of freedom. It is to be noted that, in these studies, the contributions from the basepair and the basestep degrees of freedom to the overall hole-transfer process cannot be separated and the results tend to present more of an average feature. The aim of this study, which is divided into two parts, is to estimate the energetics of the basepair deformations and then to understand their individual effects on the charge transfer (hole transfer) processes at the basestep level of DNA. We believe that an understanding of the deformations at the basepair level would prove useful in understanding the DNA–protein interactions, charge-transfer experiments, and DNA-mediated chemical reactions.

2. Methodology

2.1. Models and Calculations. To estimate the range of basepair deviations in DNA structures, we analyzed 22 B-DNA and 31 A-DNA crystal structures, totaling 72 A:T basepairs and 91 G:C basepairs. For our crystal database analysis, we have used the same set of DNA structures used to define the standard reference frame for the description of nucleic acid basepair geometry by the X3DNA program.²⁴ The population analysis for all the basepairs in the chosen crystal structures was done against individual basepair parameters. For the translational parameters [stagger (S_z), stretch (S_y) and shear (S_x)], we have used a step size of 0.025 Å, while for rotational parameters, we have used a step size of 1°. These step sizes allow us to sample the population of the individual degrees of freedom accurately.

The Gaussian 03 program has been used for the ab-initio molecular orbital calculations and the potential energy analysis. Electron correlation was accounted for using the second-order Moller–Plesset perturbation method (MP2) at the 6-31++G(d,p) basis set level.^{25,26} The choice of the method is based on the success of MP2 level of theory in describing the H-bonding interactions in DNA basepairs and organic systems.¹⁴ The DNA basepair geometries for the current study were generated using the X3DNA program, which makes use of the recommended reference frame for the description of nucleic acid basepair geometry and a rigorous matrix-based scheme to calculate local

conformational parameters.²⁴ The hydrogen positions in the basepair geometries generated using X3DNA were then relaxed by keeping all the non-hydrogen atoms frozen to the generated coordinates.

2.2. Charge Transfer. To estimate the extent of charge transfer through DNA basepairs, we evaluate the charge transfer integral between the bases as a function of all the six degrees of freedom. We describe the charge transfer via the H-bonds in the DNA basepairs by the tight-binding Hamiltonian, which is given by

$$H = \sum_i \varepsilon_i(r, \theta) a_i^\dagger a_i + \sum_{\substack{ij \\ i \neq j}} J_{ij}(r, \theta) (a_i^\dagger a_j + hc) \quad (1)$$

where a_i^\dagger and a_i are the creation and annihilation operators of a charge at the i th nucleobase, $\varepsilon_i(r, \theta)$ is the site energy of the charge, and $J_{ij}(r, \theta)$ is the charge transfer integral involving molecular orbitals, ϕ_i 's, on the nucleobases i and j . In eq 1, both the site energies and the charge transfer integrals depend on the translational (r) and rotational (θ) degrees of freedom.

The wave function of a hole can be written as a linear superposition of the highest occupied molecular orbitals (HOMOs) on the individual nucleobases. The site energies and charge-transfer integrals in eq 1 were obtained by utilizing a unique feature of the ADF program,²⁷ namely, the possibility to exploit the molecular orbitals of the nucleobases, ϕ_i (fragment orbitals), as a basis set in calculations on a system consisting of two or more nucleobases. Thus, we note that, using this feature, we can change the basis from an atomic orbital basis to the fragment orbital basis, where a fragment consists of atoms in a nucleobase. The advantage of this method is that now the overlap matrix is evaluated as the overlap between molecular orbitals of individual nucleobases. The standard output of the ADF program provides the overlap matrix, \mathbf{S} , the eigenvector matrix, \mathbf{C} , and the eigenvalue matrix, \mathbf{E} , in the fragment orbital basis. Thus, now using the generalized unitary transformation ($h_{KS} = \text{SCEC}^{-1}$) we can readily evaluate the matrix elements of the Kohn–Sham Hamiltonian, $\langle \phi_i | h_{KS} | \phi_j \rangle$. This procedure allows direct calculations of the charge-transfer integrals, including their signs, without invoking the assumption of zero spatial overlap. Therefore, it is not necessary to apply an external electric field to bring the site energies of different nucleobases into resonance. This methodology has been successfully used earlier to describe hole transfer in DNA stacks.^{7,9}

The DFT calculations were performed with an atomic basis set of Slater-type orbitals (STOs) of triple- ζ quality including two sets of polarization functions on each atom (TZ2P basis set in ADF).²⁸ The asymptotically corrected exchange correlation potential SAOP (statistical average of orbital potentials) was used in the DFT calculations.²⁹ It has been shown earlier that this potential yields reliable results both for the relative ionization energies of isolated nucleobases and for the relative site energies of G nucleobases in DNA stacks.³⁰ We also calculate the generalized charge transfer integral using the Lowdin transformation, which gives us the generalized charge transfer integrals in the orthogonal basis:

$$J'_{ij} = J_{ij} - S_{ij}(J_{ii} + J_{jj})/2 \quad (2)$$

For the dinucleotide steps, the reference geometry and the steps with distortions were generated using the X3DNA program. The reference geometry was generated with average values of basepair degrees of freedom for the B-DNA structure as described in ref 12 (note that for the rise a value of 3.38 Å was used). The maximum allowed values for the positive and

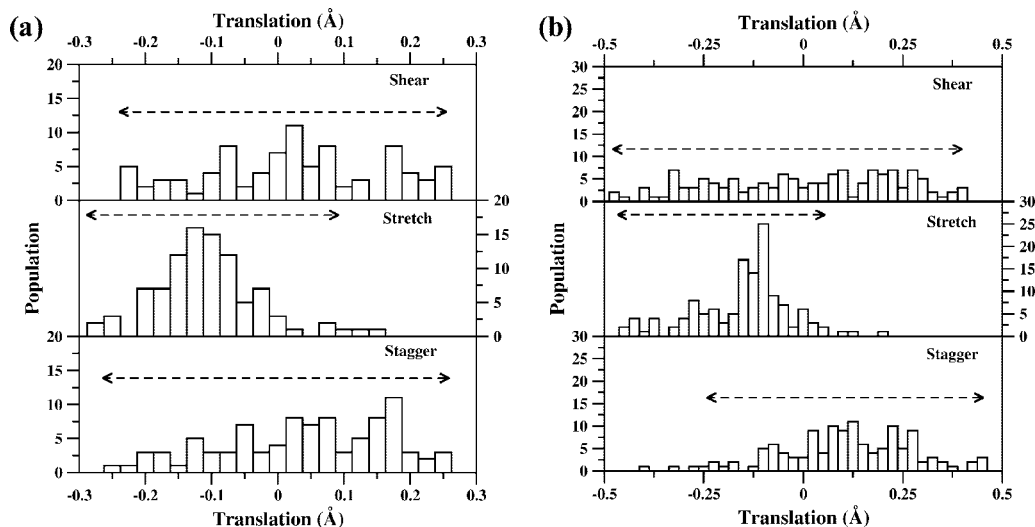


Figure 2. Population analysis for the translational degrees of freedom for the (a) A:T and (b) G:C basepairs. A step size of 0.025 Å has been used to evaluate the population distribution. Arrows are indicative of the range of the distribution.

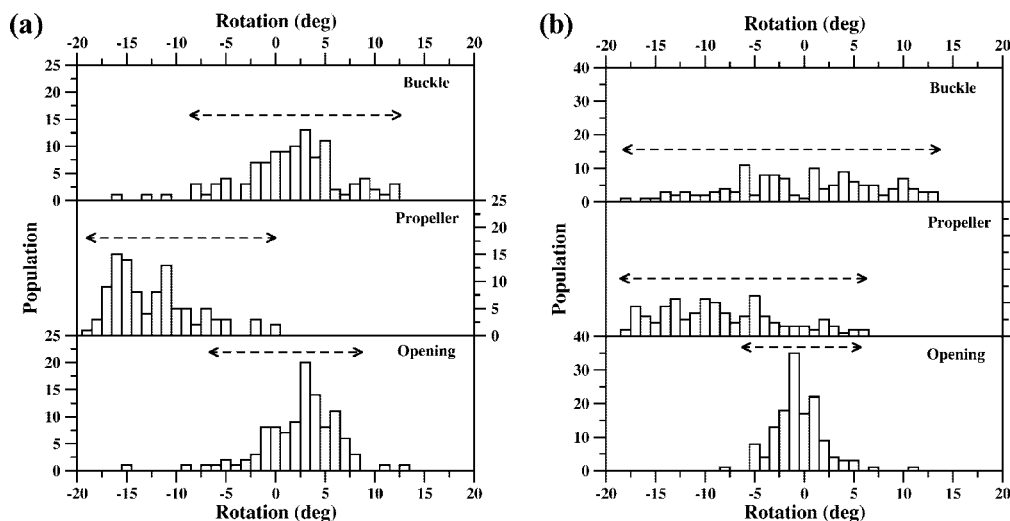


Figure 3. Population analysis for the rotational degrees of freedom for the (a) A:T and (b) G:C basepairs. A step size of 1° has been used to evaluate the population distribution. Arrows are indicative of the range of the distribution.

negative distortions of each degree of freedom were estimated from the population analysis.

3. Results and Discussion

3.1. Population Analysis. Before studying the energetics of the basepair deformations, we study the distribution of the basepair degrees of freedom in a set of 22 B-DNA and 31 A-DNA crystal structures, totaling 72 A:T basepairs and 91 G:C basepairs. This allows us to choose the range for studying the energetics of the degrees of freedom. The population analysis for the translational and rotational degrees of freedom for both the A:T and G:C basepairs are presented in Figures 2 and 3, respectively. For the A:T basepairs, we find that the translational degrees of freedom are distributed from -0.3 to 0.3 Å, while for the G:C basepairs, they are distributed between -0.5 and 0.5 Å. For both the A:T and G:C basepairs, we find that the shear (S_x) and stagger (S_z) degrees of freedom are uniformly distributed over the entire range, while stretch (S_y) is centered around -0.13 Å. This indicates that, shear (S_x) and stagger (S_z) are allowed degrees of freedom in the B-DNA and A-DNA structures. However, stretch (S_y) is a restricted degree of freedom, which can be understood by the fact that a stretching

motion leads to the dissociation of the DNA duplex structure, while the other two motions do not effect the DNA duplex structure adversely.

For both the A:T and G:C basepairs, we find that the range from -20° to 20° covers the distribution of the rotational degrees of freedom. Interestingly, we find that buckle (κ) is uniformly distributed about 0° , while propeller twist (ω) follows an asymmetric distribution and takes values only between -20° and 0° . However, we find that open (σ) is strongly centered around 2.7° for the A:T basepairs (Figure 3a) and around -1.2° for the G:C basepairs (Figure 3b). Thus, we note that open (σ) is a restricted degree of freedom in the B-DNA and A-DNA structures, which can be understood by the fact that an opening motion leads to the displacement of a nucleobase from the helical stack, thus disrupting the duplex structure.

From the population analysis, we obtain an overall picture of the distributions of the degrees of freedom in A:T and G:C basepairs. We find that while shear (S_x), stagger (S_z), buckle (κ), and propeller twist (ω) are allowed degrees of freedom, with fluctuations distributed over a large translational and rotational range, stretch (S_y) and open (σ) are restricted degrees of freedom with very limited fluctuations. To understand the

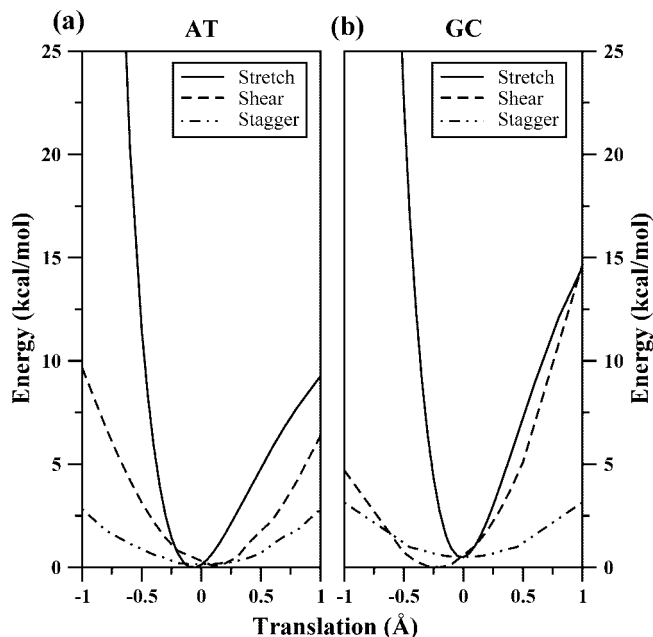


Figure 4. Potential energy profiles for the translational degrees of freedom for the (a) A:T and (b) G:C basepairs. Distances are reported in angstroms and energy in kilocalories/mole.

energetics governing these distributions, we evaluate the potential energy profile corresponding to each degree of freedom.

3.2. Potential Energy Analysis. The potential energy analysis gives us an insight into the stiffness of a particular translational or rotational mode. A flat potential profile indicates a soft mode, while a steep potential profile indicates a stiffer mode of vibration. To evaluate the potential energy profile, we scan the potential energy profile over an extended range from -1.0 to 1.0 Å for the translational degrees of freedom and from -15° to 15° for the rotational degrees of freedom.

In Figure 4, we present the potential energy profiles for the translational degrees of freedom for both the A:T (Figure 4a) and G:C (Figure 4b) basepairs. As can be clearly seen, the stagger (S_z) mode is the softest mode when compared to either stretch (S_y) or shear (S_x) for both the basepairs, with energetic costs of only up to 2.5 kcal/mol for displacements as large as 1 Å. This is intuitive because stagger (S_z) involves an out of plane motion of the bases from the equilibrium in-plane geometry, which retains the H-bonding with favorable energetics. Also, as can be seen, the potential energy profile is symmetric about 0 Å, clearly indicating that the stagger motion in either the $+z$ or the $-z$ direction is equally favored. On the other hand, we find that the potential energy profile for stretch (S_y) is asymmetric about an equilibrium value of 0 Å. For both the A:T and G:C basepairs, we find that the potential energy profile for stretch (S_y) follows the Morse potential, which has been reported earlier.³¹ From the steepness of the potential profile, it is clear that this is a very rigid mode, the rigidity of the mode being greater for the G:C basepair. This also explains the population distribution centered around -0.13 Å for both the basepairs. We find that the potential profile for shear (S_x) is asymmetric and centered around an equilibrium value of 0.1 Å for the A:T basepair and -0.2 Å for the G:C basepair. The asymmetry in the potential profile arises due to the in-plane motion of the bases, which disrupts the H-bonding. The energy cost associated with shear (S_x) is intermediate to that between stagger (S_z) and stretch (S_y), thus making the mode stiffer than stagger (S_z) and softer than stretch (S_y).

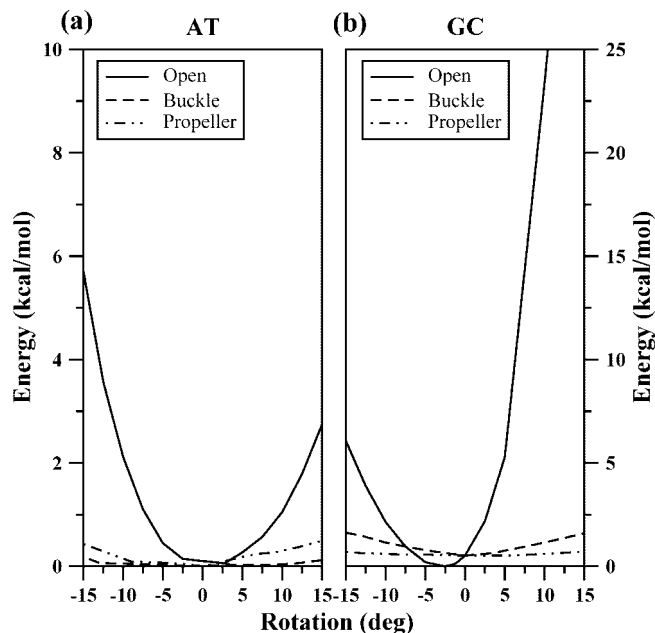


Figure 5. Potential energy profiles for the rotational degrees of freedom for the (a) A:T and (b) G:C basepairs. Angles are reported in degrees and energy in kilocalories/mole.

In Figure 5, we present the potential energy profiles for the rotational degrees of freedom for both the A:T (Figure 5a) and G:C (Figure 5b) basepairs. For both the basepairs, the propeller twist (ω) and buckle (κ) are found to be soft modes with symmetric potential profiles centered at 0° . The energy cost for fluctuations as large as 15° are found to be less than 1 kcal/mol. On the other hand, for open (σ), we find an asymmetric potential profile centered at 2.7° and -2.5° for the A:T and G:C basepairs, respectively. The mode is found to be rigid for both the basepairs when compared to the propeller twist (ω) and buckle (κ). This rigidity also explains the population distribution shown in Figure 3.

To quantify the rigidity of the modes, we calculate the force constant associated with each mode by fitting the potential energy profile around the equilibrium value to a harmonic potential ($E = (1/2)kx^2$, where k is the force constant). Even though all the modes do not sample a harmonic potential well around the equilibrium values, with some of the modes sampling an inharmonic potential well, this method is a good approximation to obtain the force constants associated with each mode.¹⁹ The force constants obtained from the harmonic fitting are summarized in Table 1. As can be seen, the force constants obtained by us replicate the general trend obtained by previously calculated results, which were evaluated from molecular dynamics trajectories. However, the magnitudes of the force constants evaluated by us are slightly lower than the previously calculated results (summarized in Table 1), because of the fact that, in the molecular dynamics runs, each basepair is flanked by surrounding basepairs that further stiffens the vibrational mode, thus increasing the magnitude of the force constant. However, on average, we notice that the G:C basepair is stiffer than the A:T basepair. We also notice that the translational degrees of freedom are stiffer in comparison to the rotational degrees of freedom. We can differentiate between the stiffness of the A:T and G:C pairs for the individual translational modes by evaluating the ratio of the force constants. This ratio (GC/AT) for the shear (S_x), stretch (S_y), and stagger (S_z) modes turns out to be 1.61, 2.15, and 1.19, respectively. Thus, we note that while the shear (S_x) and stretch (S_y) are comparatively more stiff in G:C than

TABLE 1: Force Constants for the Rotational and Translational Base Pair Degrees of Freedom (in kcal/mol deg² and kcal/mol Å², respectively)^a

	buckle	propeller	open	shear	stretch	stagger
AT	0.0003 (0.0066)	0.0010 (0.0098)	0.0089 (0.022)	3.0528 (8.5)	15.3863 (42)	1.1085 (4.0)
GC	0.0024 (0.0090)	0.0004 (0.0105)	0.0648 (0.085)	4.9154 (8.1)	33.0953 (72)	1.3273 (5.9)
GC-AT	—	—	—	1.6101	2.1509	1.1973

^a Force constants from ref 19 are given in parantheses for comparison purposes.

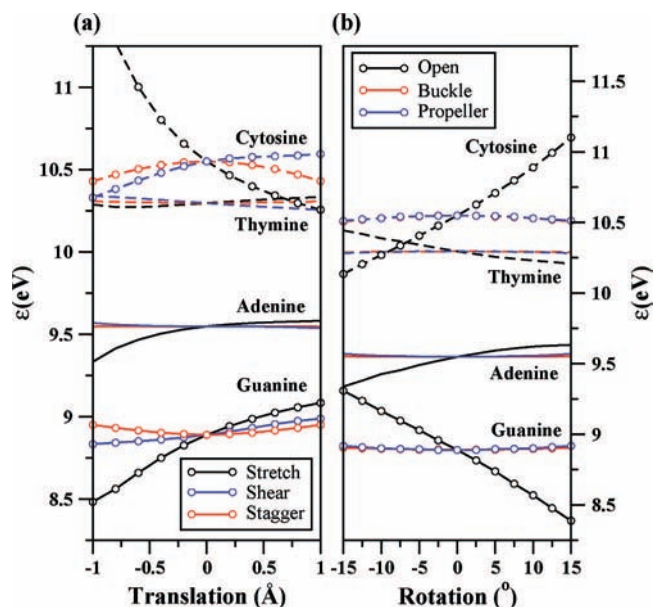


Figure 6. Site energies of the DNA bases as a function of the (a) translational and (b) rotational degrees of freedom: solid lines with circle, guanine; dashed line with circle, cytosine; solid line, adenine; dashed line, thymine. Site energies have been reported in electronvolts. Distances are reported in angstroms and angles are reported in degrees.

in A:T, there is no such preference for stagger (S_z). This result conclusively proves that base–base interactions also determine the deformity of the basepair.

3.3. Intrabasepair Charge Transfer. H-bonds in DNA basepairs are known to redistribute charges owing to the polarization of the H-bonds.³² It is known that H-bonds in proteins are responsible for charge transfer; however, in DNA, intrabasepair (A:T and G:C) charge transfer is very weak owing to large differences in the ionization potentials of the purine (adenine, guanine) and pyrimidine (cytosine, thymine) bases. The relative ionization energies (with respect to that for guanine) for isolated A, C, and T are found to be 0.20, 0.70, and 0.90 eV, respectively.³³ The large differences between the site energies of G, C and A, T bases causes the intrabasepair charge transfer to be low. However, it has been shown that in the presence of flanking bases in the 5' position, the site energies of the DNA bases fluctuate, which in some cases leads to the equalization of the site energies of the purine and the pyrimidine bases.³⁰ Thus, it becomes important to evaluate the changes in the site energies and the charge transfer integrals as a function of basepair degrees of freedom to establish which motions could affect the charge transfer.

In Figure 6 we present the variations in the site energies as a function of the translational (Figure 6a) and rotational (Figure 6b) degrees of freedom for both the purine and pyrimidine bases. For all the cases, we note that the difference in the site energies for guanine and cytosine (≈ 1.5 eV) is greater than that for adenine and thymine (≈ 0.7 eV). For the translational degrees of freedom, we note that the site energies for adenine and

thymine do not fluctuate from the equilibrium value (calculated at 0 Å shear, stretch and stagger) of 9.54 and 10.29 eV, while for guanine and cytosine, the site energies fluctuate from the equilibrium values of 8.87 and 10.55 eV, the fluctuations being larger for stretch (S_y) when compared to stagger (S_z) and shear (S_x). However, since stretch (S_y) is a restricted motion, we focus our attention on the variations in stagger (S_z) and shear (S_x), which are allowed modes of vibrations. We find that the site energies for both guanine and cytosine vary symmetrically with a variation in stagger (S_z); while the site energy for guanine gradually increases by 0.15 eV (from 8.87 to 9.02 eV), the site energy of cytosine decreases by 0.33 eV (from 10.54 to 10.21 eV) for variation in stagger (S_z) as large as ± 1 Å. On the other hand, we find that the site energies vary asymmetrically for positive and negative shear (S_x). The site energy for guanine decreases for negative shear (S_x) and increases for positive shear (S_x), the variation being on the order of 0.1 eV for both the cases. Similarly, the site energy for cytosine decreases for negative shear (S_x) and increases for positive shear (S_x), the decrease being on the order of 0.43 eV and the increase on the order of 0.17 eV. Thus, we note that the fluctuations are stronger for cytosine in comparison to guanine.

From the site energies plotted in Figure 6b, it can be seen that the site energies of the DNA bases do not vary with fluctuations in propeller twist (ω) and buckle (κ), while they show large variation with fluctuations in open (σ). However, since open is a restricted motion, these fluctuations do not effect DNA charge transfer. However, it is important to point out that both stretch (S_y) and open (σ) are responsible for controlling processes like DNA replication and enzyme selectivity. Thus, we note that an understanding of the changes in the site energies with these modes is important for gaining a deeper insight and understanding of such processes.

In Figure 7, we present the variations in the generalized charge transfer integrals as a function of the translational (Figure 7a) and rotational (Figure 7b) degrees of freedom for both the A:T and the G:C basepairs. For all the cases, we notice that the generalized charge transfer integrals for the A:T basepair are lower than that for G:C basepair. The ratio of the generalized charge transfer integrals (G:C/A:T) at the equilibrium value (all parameters set to 0) turns out to be 1.89, indicative of the cooperative effect of the H-bonds in the DNA basepairs. For the translational degrees of freedom, we find that any fluctuation in shear (S_x) and stagger (S_z) reduces the generalized charge transfer integral. On the other hand, we find that a negative stretch (S_y) increases the magnitude of the generalized charge transfer integral to values as high as 0.09 and 0.18 eV for A:T and G:C basepairs from 0.014 and 0.027 eV, respectively. The positive stretch, however, reduces the magnitude of the generalized charge transfer integral. Thus, we note that the generalized charge transfer integrals follow closely the strength of the H-bond. All the fluctuations that reduce the strength of the H-bond or lead to a loss in H-bonding reduce the magnitude of the generalized charge transfer, while those which strengthen

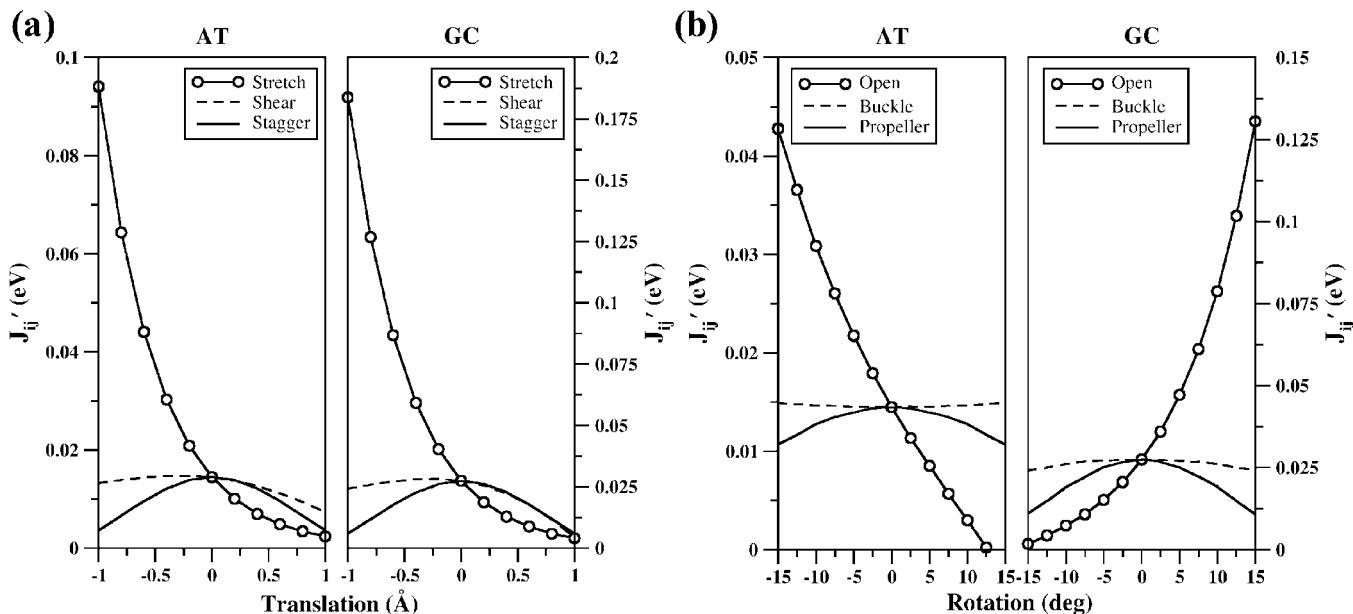


Figure 7. Generalized charge transfer integrals (J'_{ij}) for the (a) translational and (b) rotational degrees of freedom for the A:T and G:C basepairs. J'_{ij} have been reported in electronvolts. Distances are reported in angstroms and angles are reported in degrees.

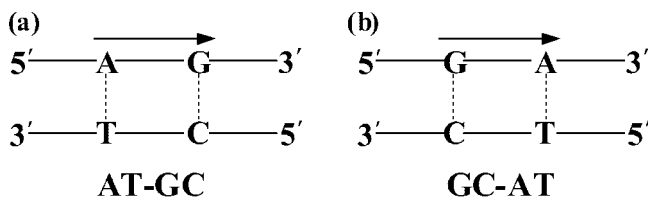


Figure 8. (a) AT–GC and (b) GC–AT dinucleotide steps considered for studying the effect of basepair deformations on charge transfer. Arrows indicate the A–G hopping and the G–A hopping in the AT–GC and GC–AT steps, respectively.

the H-bond increase the magnitude of the generalized charge transfer integrals.

It can be seen that the magnitude of the generalized charge transfer integral does not vary with fluctuations in propeller twist (ω), while it reduces for fluctuations in buckle (κ). On the other hand, the generalized charge transfer integral varies a lot with fluctuations in open (σ). For the A:T basepair, a negative open (σ) increases the generalized charge transfer integral, while a positive open (σ) reduces it. However, we find a totally complementary behavior for the G:C basepair, with an increase in the magnitude of generalized charge transfer integral for positive open (σ) and decrease with negative open (σ). This difference is again due to the strengthening and weakening of the H-bonds in the A:T and G:C basepairs for different values

of open (σ). As in the case of site energies, we again notice that large changes in the intrabasepair generalized charge transfer integral are governed by both stretch (S_y) and open (σ). This highlights the importance of these modes controlling the key processes like DNA replication and enzyme selectivity. Overall, we observe that for the range of allowed fluctuations in the basepair degrees of freedom, the intrabasepair generalized charge transfer integrals generally remain low. It is also important to point out that the magnitude of the intrabasepair generalized charge transfer integrals are smaller (0.014 eV for A:T and 0.027 eV for the G:C basepair) when compared to interbasepair generalized charge transfer integrals, which vary between 0.022 to 0.141 eV for various dinucleotide steps.⁹

3.4. Interbasepair Charge Transfer. Recent calculations have shown that the charge transfer integrals and site energies are sensitive to thermal fluctuations of the DNA structure.^{11,34} Calculations using static structures have shown that the charge transfer integrals for the dinucleotide step are strongly dependent on the twist angle (Ω) and rise (D_z).^{7,9} However, recent calculations of the charge transfer integral between dinucleotide steps (interbasepair charge transfer or intrastrand charge transfer) for a molecular dynamics trajectory, show sharp fluctuations in the charge transfer integral when compared to values computed for static structures.^{11,34} These fluctuations in the charge transfer integral have been ascribed to fluctuations in the basestep

TABLE 2: Site Energies Corresponding to Adenine and Guanine in AT–GC and GC–AT Basesteps^{a,b}

	buckle (κ)		propeller (ω)		open (σ)		stagger		stretch		shear	
distortion	–	+	–	+	–	+	–	+	–	+	–	+
	–6.50°	9.50°	–17.40°	–5.50°	–3.50°	1.50°	–0.09 Å	0.26 Å	–0.16 Å	–0.11 Å	–0.34 Å	0.26 Å
AT–GC (ϵ_G)	8.501	8.523	8.505	8.507	8.627	8.478	8.525	8.490	8.504	8.515	8.476	8.537
AT–GC (ϵ_A)	9.003	9.057	9.072	8.979	9.066	9.015	9.011	9.040	9.024	9.029	9.005	9.044
distortion	–	+	–	+	–	+	–	+	–	+	–	+
	–2.50°	4.50°	–17.50°	–11.50°	–1.50°	5.50°	–0.06 Å	0.16 Å	–0.21 Å	–0.04 Å	–0.09 Å	0.16 Å
GC–AT (ϵ_G)	8.494	8.499	8.484	8.496	8.490	8.511	8.495	8.497	8.497	8.496	8.497	8.495
GC–AT (ϵ_A)	8.969	8.966	8.983	8.968	8.947	9.007	8.948	8.975	8.964	8.970	8.968	8.965

^a Reference values: AT–GC, ϵ_G (8.502 eV), ϵ_A (9.025 eV); GC–AT, ϵ_G (8.496 eV), ϵ_A (8.967 eV). ^b Site energies have been calculated for distortions in the G:C and A:T basepairs for the AT–GC and GC–AT basesteps respectively. Maximum positive (+) and maximum negative (–) distortions for each basepair degrees of freedom evaluated from the population analysis have also been presented. All the site energies have been reported in electronvolts.

TABLE 3: Charge Transfer Integrals (J_{ij}) and the Generalized Charge Transfer Integrals (J_{ij}') for the Intrastrand G-A and A-G Hopping^{a,b}

	buckle (κ)		propeller (ω)		open (σ)		stagger		stretch		shear	
distortion	−	+	−	+	−	+	−	+	−	+	−	+
	−6.50°	9.50°	−17.40°	−5.50°	−3.50°	1.50°	−0.09 Å	0.26 Å	−0.16 Å	−0.11 Å	−0.34 Å	0.26 Å
AT–GC (J_{ij})	0.0826	0.0793	0.1109	0.0606	0.1191	0.0780	0.0884	0.0813	0.0856	0.0841	0.0343	0.1252
AT–GC (J_{ij}')	0.0296	0.0282	0.0412	0.0210	0.0439	0.0280	0.0317	0.0296	0.0311	0.0303	0.0113	0.0461
distortion	−	+	−	+	−	+	−	+	−	+	−	+
	−2.50°	4.50°	−17.50°	−11.50°	−1.50°	5.50°	−0.06 Å	0.16 Å	−0.21 Å	−0.04 Å	−0.09 Å	0.16 Å
GC–AT (J_{ij})	0.0121	0.0004	0.0044	0.0055	0.0138	0.0482	0.0114	0.0036	0.0053	0.0067	0.0209	0.0233
GC–AT (J_{ij}')	0.0043	0.0008	0.0020	0.0015	0.0058	0.0178	0.0040	0.0008	0.0014	0.0021	0.0075	0.0095

^a Reference values: AT–GC, J_{ij} (0.0854 eV), J_{ij}' (0.0310 eV); GC–AT, J_{ij} (0.0058 eV), J_{ij}' (0.0017 eV). ^b Charge-transfer integrals have been calculated for distortions in the G:C and A:T basepairs for the AT–GC and GC–AT basesteps, respectively. Maximum positive (+) and maximum negative (−) distortions for each basepair degrees of freedom evaluated from the population analysis have also been presented. All the charge transfer integrals have been reported in electronvolts.

parameters and influence of the DNA environment. However, in these studies the influence of basepair degrees of freedom on the charge transfer integrals were not discussed. It has been shown that the rate of charge transfer in DNA strands is strongly coupled to the number of (AT)_n bridges separating the donor and acceptor G:C basepairs.³⁵ There can be 10 different types of dinucleotide steps; however, to study the influence of the basepair degrees of freedom on the charge transfer integrals and site energies, we have chosen the AT–GC and the GC–AT dinucleotide steps for a detailed analysis (Figure 8). The choice of the dinucleotide steps is based on the fact that the site energies of guanine are comparable to that of adenine; thus, these steps strongly influence the hole transport in DNA (also note that intrastrand hole transfer dominates interstrand hole transfer). We evaluate the charge transfer integral for the A–G hopping in the AT–GC step and G–A hopping in the GC–AT step.

The distortions in the basepair degrees of freedom are allowed only for the 3'-basepair, while the 5'-basepair is kept fixed to the reference geometry. This is in accordance with the fact that the effect of the flanking nucleobase at the 5'-position on the site energies is much less pronounced than the effect of the nucleobase at the 3'-position.⁹ Thus, in the AT–GC basestep, we study distortions in the G:C basepair, while in the GC–AT step we study distortions in the A:T basepair. For both the basesteps, the site energies and charge-transfer integrals evaluated for distortions in basepair degrees of freedom have been summarized in Tables 2 and 3, respectively. For the AT–GC basestep, we find that the site energies of both guanine (ϵ_G) and adenine (ϵ_A) vary with the G:C basepair degrees of freedom, the fluctuations in the site energies being as high as 0.126 eV for guanine and 0.047 eV for adenine. Note that these variations in the site energies, especially for guanine, are on the same scale as that due to changing the flanking nucleobases (Table 2 of ref 9). We also find that the difference between the site energies ($\epsilon_A - \epsilon_G$) can reduce from 0.522 to 0.437 eV for an open (σ) of −3.50° of the G:C basepair and can increase to 0.567 eV for a propeller twist (ω) of −17.40°. Among the translational degrees of freedom, we find that negative stagger (S_z) and positive shear (S_x) influence the site energies of guanine, but these are weaker compared to open (σ) and propeller twist (ω). For the GC–AT basestep, we find that the site energies of guanine and adenine do not fluctuate drastically from the reference values, and the difference in the site energies remains constant. This clearly shows that variations in the A:T basepair do not influence the site energies.

Additionally, the charge transfer integral (J_{ij}) for the A–G hopping in the AT–GC step fluctuates with the basepair degrees of freedom of the G:C basepair. Interestingly, we find that the charge transfer integral varies considerably for shear (S_x),

positive shear (S_x) increasing the charge transfer integral by 0.0398 to 0.1252 eV from the reference value of 0.0854 and negative shear (S_x) reducing it by 0.0511 to 0.0343 eV. Note that the fluctuation in the charge transfer integral is comparable to the reference value itself. This behavior is more prominent for the G–A hopping in the GC–AT basestep, where the charge transfer integral can vary from 0.0036 to 0.0482 eV from the reference value of 0.0058 eV. It is interesting to note that the fluctuations in the charge transfer integral computed along the molecular dynamics trajectory are concurrent with the fluctuations observed by us.^{11,34} We find that open (σ), propeller twist (ω), and shear (S_x) strongly influence the charge transfer integrals and site energies when compared to the other degrees of freedom. Thus, our findings suggest that fluctuations in basepair degrees of freedom strongly affect the charge transfer in DNA strands.

4. Conclusions

In summary, we have investigated the energetics of the basepair degrees of freedom and their effects on the overall charge transfer processes in DNA. We find that the rotational and translational basepair degrees of freedom can be broadly classified into soft and hard vibrational modes. In fact, the nature of the basepair (A:T or G:C) also determines the stiffness of the modes. We find that the intrabasepair charge transfer, in the A:T and G:C basepairs, is influenced by the hard vibrational modes, namely open (σ) and stretch (S_y). This observation is relevant to understanding DNA processes like replication, which involves the opening of the DNA helix. At the basestep level, our calculations for the AT–GC and GC–AT dinucleotide steps suggest that fluctuations in the G:C basepair strongly influence the site energies when compared to fluctuations in the A:T basepair. However, for both the dinucleotide steps, we find that the charge transfer integrals are strongly influenced by the fluctuations at the basepair level. Among the rotational degrees of freedom, the propeller twist (ω) and open (σ) influence the overall charge transfer processes. While for the translational degrees of freedom, the shear (S_x) influences the overall charge transfer process. Overall, our studies suggest that for a better understanding of the overall charge transfer processes it is important to include the basepair fluctuations into the calculations.

Acknowledgment. We thank Dr. K. Senthilkumar for help with ADF calculations. S.S.M. thanks Divya Nayar for useful discussions. S.S.M. thanks CSIR for the SR fellowship. S.K.P. acknowledges CSIR and DST, Government of India, for the research grants.

References and Notes

- (1) Folta-Stogniew, E.; Russu, I. M. *Biochemistry* **1994**, *33*, 110616–11024.
- (2) Snoussi, K.; Leroy, J. L. *Biochemistry* **2001**, *40*, 8898–8904.
- (3) Roberts, R. J.; Halford, S. S. In *Nucleases*; Linn, S. M.; Lloyd, R. S.; Roberts, R. J., Eds.; Cold Spring Harbor Lab. Press: Plainview, NY, 1993.
- (4) Roberts, R. J. *Cell* **1995**, *82*, 9–12.
- (5) Cheng, X.; Roberts, R. J. *Nucleic Acids Res.* **2001**, *29*, 3784–3795.
- (6) Klimasauskas, S.; Kumar, S.; Roberts, R. J.; Cheng, X. *Cell* **1994**, *76*, 357–369.
- (7) Grozema, F. C.; Siebbeles, L. D. A.; Berlin, Y. A.; Ratner, M. A. *Chem. Phys. Chem.* **2002**, *6*, 536–539.
- (8) Berlin, Y. A.; Burin, A. L.; Siebbeles, L. D. A.; Ratner, M. A. *J. Phys. Chem. A* **2001**, *105*, 5666–5678.
- (9) Senthilkumar, K.; Grozema, F. C.; Guerra, C. F.; Bickelhaupt, F. M.; Lewis, F. D.; Berlin, Y. A.; Ratner, M. A.; Siebbeles, L. *J. Am. Chem. Soc.* **2007**, *127*, 14894.
- (10) Voityuk, A.; Siriwong, K.; Roesch, N. *Angew. Chem., Int. Ed.* **2004**, *43*, 624.
- (11) Kubar, T.; Woiczikowski, P. B.; Cuniberti, G.; Elstner, M. *J. Phys. Chem. B* **2008**, *112*, 7937–7947.
- (12) Dickerson, R. E. *Nucleic Acids Res.* **1989**, *17*, 1797–1803.
- (13) El Hassan, M. A.; Calladine, C. R. *Philos. Trans.: Math., Phys. Eng. Sci.* **1997**, *355*, 43–100.
- (14) Muller-Dethlefs, K.; Hobza, P. *Chem. Rev.* **1999**, *99*, 3247–3276.
- (15) Guerra, C. F.; Bickelhaupt, F. M.; Snijders, J. G.; Baerends, E. J. *J. Am. Chem. Soc.* **2000**, *122*, 4117–4128.
- (16) Drew, H. R.; Wing, R. M.; Takano, T.; Broka, C.; Tanaka, S.; Itakura, K.; Dickerson, R. E. *Proc. Natl. Acad. Sci. U.S.A.* **1981**, *78*, 2179.
- (17) Perez, A.; Noy, A.; Lankas, F.; Javier Luque, F.; Orzoco, M. *Nucleic Acids Res.* **2004**, *32*, 6144.
- (18) Lankas, F.; Sponer, J.; Langowski, J.; Cheatham, T. E. *Biophys. J.* **2003**, *85*, 2872–2883.
- (19) Lankas, F.; Sponer, J.; Langowski, J.; Cheatham, T. E. *J. Am. Chem. Soc.* **2004**, *126*, 4124–4125.
- (20) Sadowska-Aleksiejew, A.; Rak, J.; Voityuk, A. A. *Chem. Phys. Lett.* **2006**, *429*, 546–550.
- (21) Grozema, F. C.; Tonzani, S.; Berlin, Y. A.; Schatz, G. C.; Siebbeles, L. D. A.; Ratner, M. A. *J. Am. Chem. Soc.* **2008**, *130*, 5157–5166.
- (22) Siriwong, K.; Voityuk, A. A. *J. Phys. Chem. B* **2008**, *112*, 8181–8187.
- (23) Hatcher, E.; Balaeff, A.; Keinan, S.; Venkatramani, R.; Beratan, D. N. *J. Am. Chem. Soc.* **2008**, *130*, 11752–11761.
- (24) Lu, X.-J.; Olson, W. K. *Nucleic Acids Res.* **2003**, *31*, 5108–5121, and references therein.
- (25) Frisch, M. J.; Trucks, G. W.; Schlegel, H. B.; Scuseria, G. E.; Robb, M. A.; Cheeseman, J. R.; Montgomery, J. A., Jr.; Vreven, T.; Kudin, K. N.; Burant, J. C.; Millam, J. M.; Iyengar, S. S.; Tomasi, J.; Barone, V.; Mennucci, B.; Cossi, M.; Scalmani, G.; Rega, N.; Petersson, G. A.; Nakatsuji, H.; Hada, M.; Ehara, M.; Toyota, K.; Fukuda, R.; Hasegawa, J.; Ishida, M.; Nakajima, T.; Honda, Y.; Kitao, O.; Nakai, H.; Klene, M.; Li, X.; Knox, J. E.; Hratchian, H. P.; Cross, J. B.; Bakken, V.; Adamo, C.; Jaramillo, J.; Gomperts, R.; Stratmann, R. E.; Yazyev, O.; Austin, A. J.; Cammi, R.; Pomelli, C.; Ochterski, J. W.; Ayala, P. Y.; Morokuma, K.; Voth, G. A.; Salvador, P.; Dannenberg, J. J.; Zakrzewski, V. G.; Dapprich, S.; Daniels, A. D.; Strain, M. C.; Farkas, O.; Malick, D. K.; Rabuck, A. D.; Raghavachari, K.; Foresman, J. B.; Ortiz, J. V.; Cui, Q.; Baboul, A. G.; Clifford, S.; Cioslowski, J.; Stefanov, B. B.; Liu, G.; Liashenko, A.; Piskorz, P.; Komaromi, I.; Martin, R. L.; Fox, D. J.; Keith, T.; Al-Laham, M. A.; Peng, C. Y.; Nanayakkara, A.; Challacombe, M.; Gill, P. M. W.; Johnson, B.; Chen, W.; Wong, M. W.; Gonzalez, C.; Pople, J. A. *Gaussian 03, revision B.05*; Gaussian, Inc.: Wallingford, CT, 2004.
- (26) (a) Moller, C.; Plesset, M. S. *Phys. Rev.* **1934**, *46*, 618. (b) Head-Gordon, M.; Pople, J. A.; Frisch, M. J. *Chem. Phys. Lett.* **1988**, *153*, 503.
- (27) (a) Bickelhaupt, F. M.; Baerends, E. J. In *Reviews on Computational Chemistry*; Lipkowitz, K. B., Boyd, D. B., Eds.; Wiley-VCH: New York, 2000; Vol. 15, pp 1–86. (b) Te Velde, G.; Bickelhaupt, F. M.; Baerends, E. J.; Fonseca Guerra, C.; Van Gisbergen, S. J. A.; Snijders, J. G.; Ziegler, T. *J. Comput. Chem.* **2001**, *22*, 931–967.
- (28) Snijders, J. G.; Vernooijs, P.; Baerends, E. J. *At. Data Nucl. Data Tables* **1981**, *26*, 483–509.
- (29) Chong, D. P.; Gritsenko, O. V.; Baerends, E. J. *J. Chem. Phys.* **2002**, *116*, 1760–1772.
- (30) Senthilkumar, K.; Grozema, F. C.; Guerra, C. F.; Bickelhaupt, F. M.; Siebbeles, L. D. A. *J. Am. Chem. Soc.* **2003**, *125*, 13658–13659.
- (31) Mallajosyula, S. S.; Datta, A.; Pati, S. K. *Synth. Met.* **2005**, *155*, 398–401.
- (32) (a) Jeffrey, G. A.; Saenger, W. *Hydrogen Bonding in Biological Structures*; Springer: Berlin, 1991. (b) Desiraju, G. R.; Steiner, T. *The Weak Hydrogen Bond in Structural Chemistry and Biology*; Oxford University Press, Oxford, 1999.
- (33) Hush, N. S.; Cheung, A. S. *Chem. Phys. Lett.* **1975**, *34*, 11.
- (34) Voityuk, A.; Siriwong, K.; Rosch, N. *Angew. Chem., Int. Ed.* **2004**, *43*, 624.
- (35) Schuster, G. B., Ed. *Long-Range Charge Transfer in DNA I-II: Topics in Current Chemistry*; Springer: Heidelberg, 2004.